PHILOSOPHICAL TRANSACTIONS OF THE ROYAL SOCIETY A MATHEMATICAL, PHYSICAL & ENGINEERING SCIENCES

Acoustic Microscopy of Surface Cracks [and Discussion]

J. M. Rowe, J. Kushibiki, M. G. Somekh, G. A. D. Briggs, C. B. Scruby, D. P. Almond, R. B. Thompson and H. N. G. Wadley

Phil. Trans. R. Soc. Lond. A 1986 **320**, 201-214
doi: 10.1098/rsta.1986.0111

Phil. Trans. R. Soc. Lond. A **320**, 201–214 (1986)
Printed in Great Britain

Acoustic microscopy of surface cracks

By J. M. Rowe, J. Kushibiki†, M. G. Somekh and G. A. D. Briggs
University of Oxford, Department of Metallurgy and Science of Materials, Oxford OX1 3PH, U.K.

[Plates 1 and 2]

The uniqueness of the acoustic microscope lies in its ability to image the way in which acoustic waves interact with the elastic properties of a specimen with microscopic resolution. A dominant role in the contrast achieved is played by Rayleigh waves that are excited in the surface of the specimen. They enable very fine surface cracks to be imaged, because they can strike them from the side and be strongly scattered. To account for this theoretically, the imaging theory of the acoustic microscope must be extended to account for non-specular scattering due to the crack. Experiments have been conducted using a cylindrical line-focus lens to measure the signal from a crack in glass, and the results can be compared directly with two-dimensional calculations from the theory. Applications of the ability of the microscope to image microscopic surface cracks include the analysis of metal fatigue and inspection of engineering ceramics, and the theoretical analysis may provide the basis for eventually characterizing surface microcracks quantitatively.

1. The phenomenon

1.1. *Acoustic microscopy*

The uniqueness of acoustic microscopy lies in the ability to image the way in which acoustic waves interact with the elastic properties of a specimen. In some cases, the penetration of ultrasonic waves through opaque materials is exploited in order to image defects that lie approximately one millimetre below a surface; this may be considered as high resolution ultrasonic NDT, and can be readily achieved at frequencies up to 60 MHz, at which the resolution is about 0.1 mm (Smith *et al.* 1985). At higher frequencies, and this will apply to all the results to be described here, acoustic microscopy is essentially a surface-imaging technique, and the contrast arises primarily from factors that affect the propagation of Rayleigh waves in the surface of the specimen.

The principle of the scanning acoustic microscope is becoming increasingly well known (Lemons & Quate (1979); for a general introduction to the technique and its applications, see Briggs (1985)). The heart of the instrument is the lens, which consists of a spherical surface, ground in the centre of one face of a sapphire disc, and coated with a quarter-wave acoustic-impedance matching layer. On the other face of the disc, opposite the lens, there is a zinc oxide transducer, and this is connected to appropriate RF circuitry. An RF pulse is applied to the transducer; this generates an acoustic pulse that travels through the sapphire and is refracted at the spherical surface to form focused waves in the coupling fluid, which is usually warm water. Because the refractive index for acoustic waves passing from sapphire to water is very large (about 7.4), spherical aberrations are generally negligible, and the focal-spot size

† Permanent address: Department of Electrical Engineering, Tohoku University, Sendai 980, Japan.

is limited almost entirely by diffraction, to about a wavelength across. Some of the energy is reflected by the specimen and passes back through the lens to the transducer, where it produces an electric signal, which again is appropriately amplified and measured to give a value for the acoustic reflection from that point on the specimen surface. In order to build up a picture, the lens is mechanically scanned in a plane parallel to the specimen surface, and the reflection from each point is stored (often digitally) and displayed on a monitor. Because the resolution is determined primarily by the wavelength used, by increasing the frequency the resolution can be improved correspondingly, the ultimate limitation being attenuation in the coupling fluid. Thus, for example, at 3 GHz the resolution in water is 0.5 μm, i.e. about the wavelength of light. The highest resolution that has been achieved in a water-coupled acoustic microscope is 0.2 μm (Hadimioglu & Quate 1983); the images described in this paper that were taken at 0.73 GHz have a resolution of 2 μm.

1.2. *Rayleigh waves*

The contrast in acoustic micrographs must not be interpreted naïvely; a bright (or dark) region cannot simply be identified as having high (or low) modulus (or density). Rather, it is necessary to understand how the contrast varies as the defocus is changed. This has become known as $V(z)$ (Quate *et al.* 1979), V referring to the voltage of the transducer signal, and z to the distance between the focal plane and the surface of the specimen (by convention, when the specimen is moved towards the lens z is taken as negative). If the imaging scan of a microscope is turned off, and with the lens above one spot on the specimen the lens is scanned along its axis, a $V(z)$ curve may be measured. The chief features of this curve are a peak signal corresponding to focus, and a series of oscillations in $V(z)$ as the specimen is moved closer to the lens. These oscillations have a regular spacing, which is related to the Rayleigh-wave angle by

$$\Delta z = \tfrac{1}{2}\lambda/\{1-\cos\theta_{\mathrm{R}}\}, \tag{1}$$

where λ is the wavelength in the coupling fluid. The Rayleigh angle, θ_{R}, is the angle of incidence of plane waves in the water for maximum excitation of Rayleigh waves in the surface of the solid, and is given by Snell's law as

$$\sin\theta_{\mathrm{R}} = v/v_{\mathrm{R}} \tag{2}$$

where v is the velocity in the water and v_{R} is the Rayleigh velocity. Equation (1) has now been extensively verified both by using a conventional spherical lens (Weglein 1979) and, more recently, by using a cylindrical lens (Kushibiki & Chubachi 1985). The oscillations may be thought of as being due to the interference of two rays. The first is normal to the surface of the specimen, and the second is incident on the specimen at the Rayleigh angle. As the defocus is changed, the path lengths of these two rays change at different rates, leading to the periodicity described by (1). This quantitative agreement is very important, and it demonstrates the dominant role played by Rayleigh waves in the contrast of the acoustic microscope.

1.3. *Surface-crack images*

Generally, little contrast is seen in the acoustic microscope when a specimen is at focus. The most interesting contrast is usually seen when the specimen is defocused a little towards the lens, because this enhances the interference between the normal and Rayleigh reflections. The

PHILOSOPHICAL TRANSACTIONS OF THE ROYAL SOCIETY A MATHEMATICAL, PHYSICAL & ENGINEERING SCIENCES

microscope then becomes sensitive to anything that affects the propagation of the Rayleigh waves excited in the surface. Thus, for example, good contrast can be found from variations in isotropic elastic properties of a specimen, from the anisotropy of grains in a polycrystalline material, or from perturbation of the Rayleigh velocity by surface layers. Damping and scattering mechanisms can attenuate the Rayleigh waves, and also give rise to contrast. The particular phenomenon considered here is the contrast from surface-breaking cracks. Suppose that these are very fine, much less than a wavelength wide, then incident waves that are geometrically reflected from the surface will be only very slightly affected by the crack and, if the crack is sufficiently narrow, it will not be detectable at all by this means. Thus, for example, in light microscopy a crack that is finer than the resolution limit will not normally be detectable. But in acoustic microscopy the Rayleigh waves which play such an important role in the contrast can strike such a crack from the side and be strongly scattered however fine it is. Thus good contrast can be obtained even from cracks that are much narrower than the resolution limit (Ilett *et al.* 1984).

In figure 1, plate 1, optical (*a*) and acoustic (*b*) images are presented of a section through an Al–Si plain-bearing alloy. The two pictures are of the same area at the same magnification; the material to the left of each picture is the steel substrate. The specimen had been tested to incipient fatigue failure, and was being examined for fatigue cracks. It is difficult to find the cracks in the optical image at this magnification, although when located it was possible to see them at higher optical magnification ($\times 400$). In the acoustic image they are rather easier to find. Some idea of how fine such cracks can be and still be imaged acoustically can be gained from the acoustic and scanning electron images in figure 2, plate 1. This specimen is a hard-metal cutting tool that has been coated with TiN by chemical vapour deposition. As it cools down from the coating process the substrate contracts more than the TiN, and thermal stress relief cracking occurs. The cracks appear in this acoustic image (*a*) as a network of bright lines, although by changing the defocus the contrast may reverse. These cracks are not visible in any other kind of microscopy at this magnification, and so, for location, some hardness indents were made (after the cracks had formed). The SEM image (*b*) is of the area around the indent in the top centre of the acoustic image, and it suggests that the width of the crack at the surface is approximately 0.1 μm, certainly much less than an acoustic wavelength wide. Indeed, the wavelengths in the coupling fluid of the waves used to form the acoustic image were the same length as the 2 μm marker of the SEM image. This would certainly not give adequate contrast from geometrical reflection from the exposed mouth of such a fine crack, so that the extraordinarily strong acoustic contrast must indeed come from the scattering of Rayleigh waves in the specimen that can strike the crack broadside.

2. Theoretical analysis

2.1. *Formulation*

The conventional theory for the variation of contrast is written as an integral of the product of a function $L(k_x)$ describing the properties of the lens and the reflectance function $R(k_x)$ of the specimen, over all angles of incidence; k_x being the component of the wavevector parallel to the specimen surface. For any value of z other than focus there is an additional phase shift within the integral, equal to twice the dot product of the incident wavevector and the amount

of defocus. This gives, in two dimensions, with k_z as the component of the wavevector normal to the surface

$$V(z) = \int_{-\infty}^{\infty} L(k_x)\, R(k_x)\, \exp(2ik_z z)\, \mathrm{d}k_x. \tag{3}$$

This expression for $V(z)$ is very robust and has been extensively tested. However, there is a serious problem in applying it to the contrast arising from surface cracks. The function $R(k_x)$ is defined for infinite plane waves that are reflected into infinite plane waves at the reflected angle, and is not capable of describing any scattering that may occur as a result of variations within planes parallel to the surface. To overcome this problem the incident wavefield and the returning wavefield must be summed separately. If the incident wavevectors are written primed, the lens is characterized for transmitting by $L_1(k'_x)$, and the coordinate system is defined with the crack in the plane $x = 0$ and the lens axis at $x = -x_0$, then the wave field incident on the specimen is

$$\phi_i(k'_x) = L_1(k'_x)\, \exp[\mathrm{i}(k'_z z + k'_x x_0)]. \tag{4}$$

It is now necessary to describe how this will be scattered by a crack. For this purpose it is useful to separate the reflectance function of a defect-free surface into two parts by an identity that defines $R_0(k_x)$ (Bertoni 1984):

$$R(k_x) \equiv R_0(k_x)\, [1 + (k_\mathrm{p}^2 - k_0^2)/(k_x^2 - k_\mathrm{p}^2)], \tag{5}$$

where k_p is the pole of the reflectance function that describes the phenomena associated with the excitation of Rayleigh waves; in the absence of attenuation in the solid k_0 is the complex conjugate of k_p. Around this pole $R_0(k_x)$ is almost exactly equal to one, and so, to a good approximation

$$R(k_x) \approx R_0(k_x) + (k_\mathrm{p}^2 - k_0^2)/(k_x^2 - k_\mathrm{p}^2). \tag{6}$$

The advantage of separating the reflectance into these two terms is that the first term may be considered as describing the geometrical reflection from the specimen surface, and the scattering of the Rayleigh wave by the crack can be accounted for in terms of its effect on the second term alone. This enables the scattering of an incident wavevector, k'_x, into a returning wavevector, k_x, to be described by a Green function in k-space (Somekh *et al.* 1985):

$$S(k_x, k'_x) = R_0\, \delta(k_x - k'_x) + \frac{2\alpha}{\pi} \left\{ \left[\frac{(T-1-R)\, k_x k'_x + (T-1+R)\, k_\mathrm{p}^2}{(k_x^2 - k_\mathrm{p}^2)\, (k_x'^2 - k_\mathrm{p}^2)} \right] + \mathrm{i}\pi\delta(k'_x - k_x)\, k_\mathrm{p} \left[\frac{1}{k_x^2 - k_\mathrm{p}^2} + \frac{1}{k_x'^2 - k_\mathrm{p}^2} \right] \right\}, \tag{7}$$

where δ is the Dirac delta function. This gives the reflected field at the surface of the specimen as

$$\phi_\mathrm{r} = S(k_x, k'_x)\, \phi(k'_x). \tag{8}$$

Description of plate 1

Figure 1. A plain bearing that has been tested for fatigue failure. The optical (*a*) and acoustic (*b*) images are of the same area at the same magnification. At the left is the steel substrate, in the centre is the Al–20 % Si bearing alloy containing the fatigue cracks. The acoustic image was taken at 0.73 GHz.

Figure 2. A hard metal cutting tool, coated with TiN. A region in the top centre of the acoustic image (*a*) is shown at 25 times greater magnification in the SEM image (*b*). The acoustic image was taken at 0.73 GHz, at this frequency the wavelength in water is 2 μm.

PHILOSOPHICAL TRANSACTIONS OF THE ROYAL SOCIETY A MATHEMATICAL, PHYSICAL & ENGINEERING SCIENCES

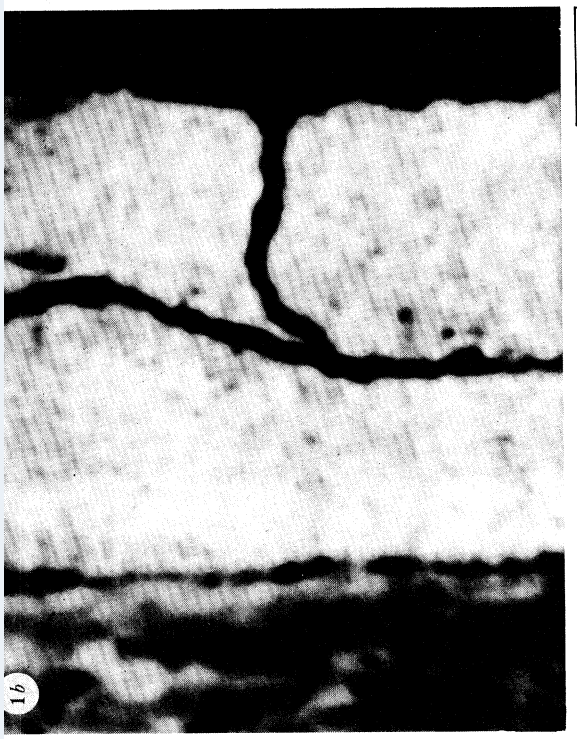

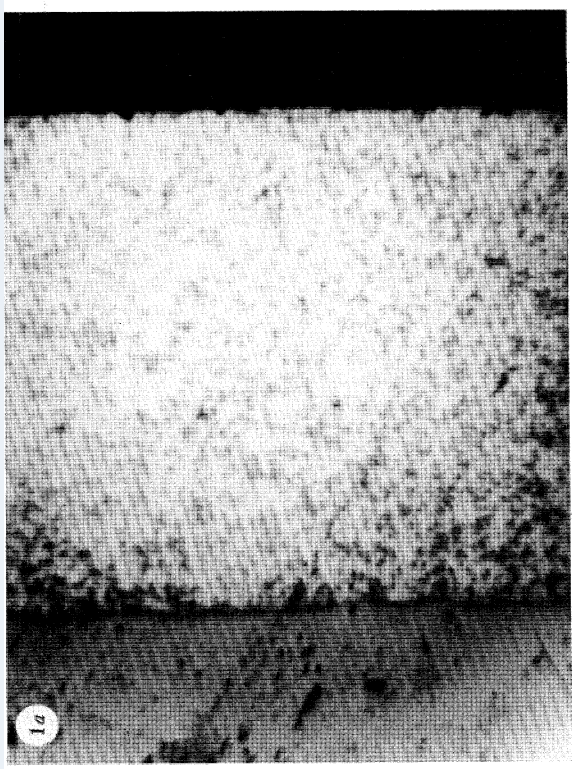

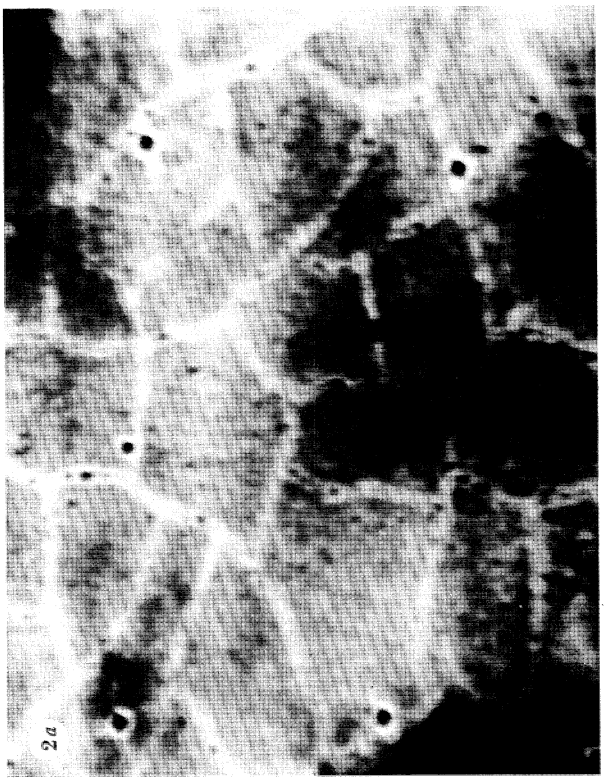

PLATE 1. For description see opposite.

(*Facing p.* 204)

PHILOSOPHICAL TRANSACTIONS OF THE ROYAL SOCIETY A MATHEMATICAL, PHYSICAL & ENGINEERING SCIENCES

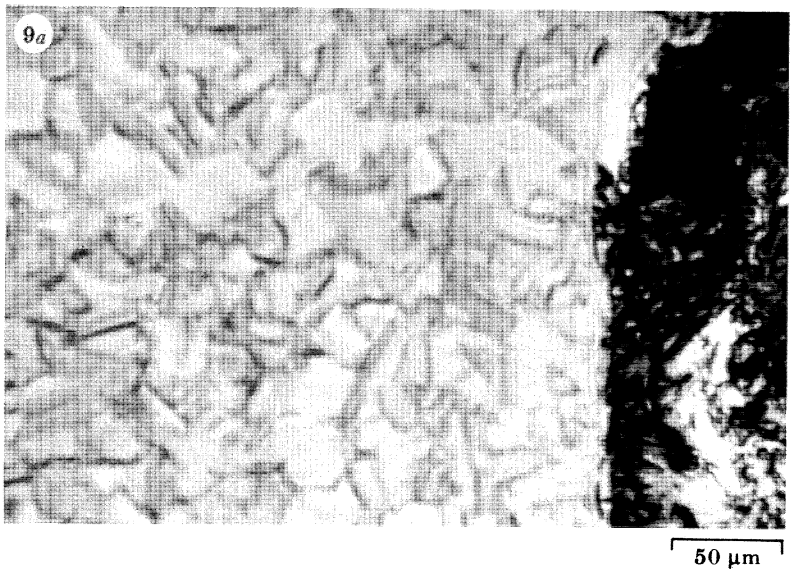

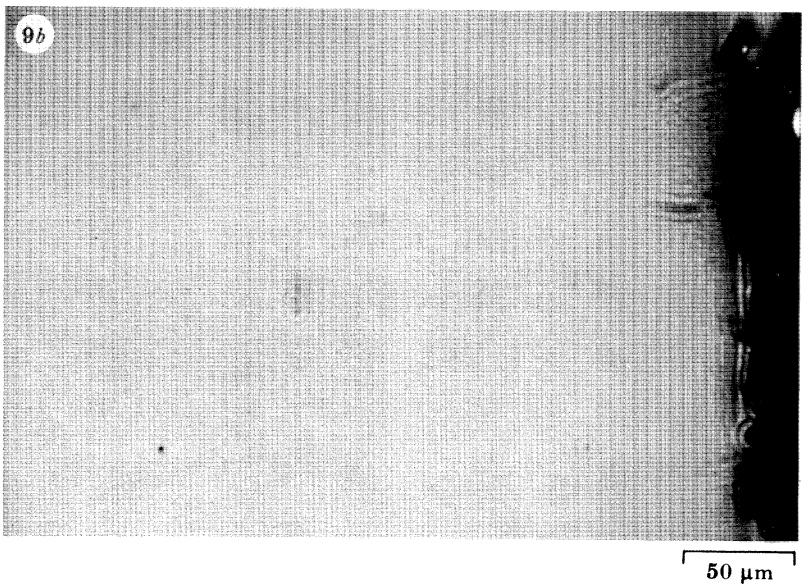

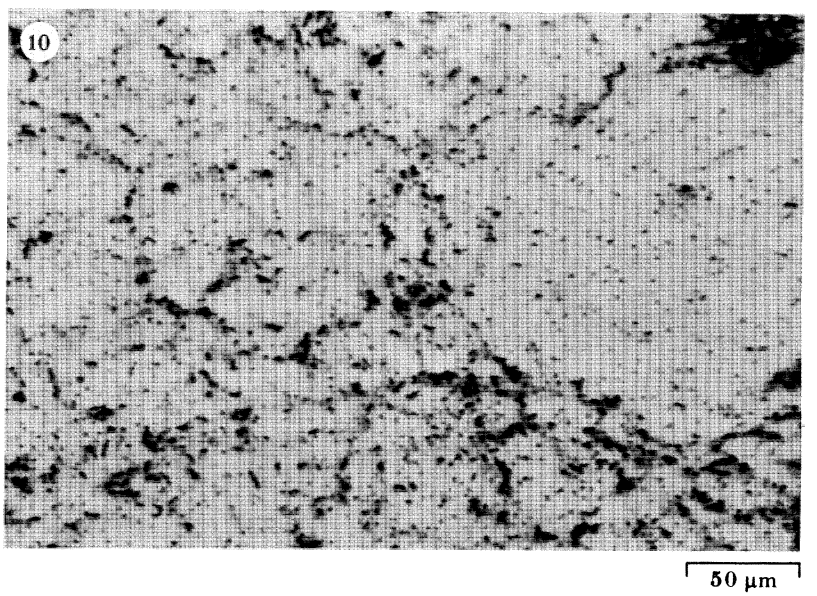

FIGURE 9. Fatigued 316 stainless steel, acoustic micrographs at 0.37 GHz: (*a*) $z = -20$ μm; (*b*) $z = +32$ μm.
FIGURE 10. Zirconia toughened alumina, acoustic image at 0.37 GHz.

PHILOSOPHICAL TRANSACTIONS OF THE ROYAL SOCIETY A MATHEMATICAL, PHYSICAL & ENGINEERING SCIENCES

A similar summation is now performed to that for the incident field, letting L_2 characterize the lens for receiving, to give the final signal from the transducer:

$$V(z) = \int_{-\infty}^{\infty} \int_{-\infty}^{\infty} L_2(k_x) \exp[\mathrm{i}(k_z z - k_x x_0)]\, S(k_x, k_x')\, L_1(k_x') \exp[\mathrm{i}(k_z' z + k_x' x_0)]\, \mathrm{d}k_x'\, \mathrm{d}k_x. \quad (9)$$

2.2. *Calculated results*

This expression enables the microscope signal to be calculated as a function of the defocus for any displacement of the lens relative to the crack. There are two sets of parameters to be determined for such a calculation: the parameters L that characterize the lens, and the transmission and reflection coefficients of the crack to be used in S. The problem of experimental characterization of the lens of an acoustic microscope has still not been satisfactorily solved at the frequencies used here. Therefore, to guide the calculations, $V(z)$ was measured with a cylindrical lens on a specimen of polished lead. Lead was used because Rayleigh waves are not excited in its surface in a water-coupled microscope; indeed the reflectance function is almost constant over most of the aperture of acoustic lenses used in practice. A simple pupil function was chosen that gave a theoretical $V(z)$ for lead that was in reasonable agreement with $V(z)$ measured experimentally. This pupil function was used in the subsequent calculations. However, this pupil function is certainly not exactly correct and so, in order to produce results that may be compared with experiment, the theoretical curves were processed by using a method that was originally developed for experimental measurements of $V(z)$ by Kushibiki & Chubachi (1985). In essence, this consists of subtracting the $V(z)$ curve for lead from the $V(z)$ curve for the given specimen. Then a fine correction is applied by suitable filtering to compensate for the difference between the lead and an ideal reflector. This yields a reduced $V(z)$ curve that should depend almost entirely on the propagation of acoustic waves in the specimen, and be substantially independent of the characteristics of the particular lens used.

Curves generated by this method are presented in figures 3–5. Figure 3*a* shows a reduced $V(z)$ curve for glass that has a uniform surface, free from any defects. The other curves are all for the same glass, but with a crack. The scattering of Rayleigh waves incident on a surface crack has been studied for the case when there is no fluid loading and the excitation is far from the crack (Achenbach *et al.* 1980), and these results may be used as an approximate description of the situation of a crack being observed in an acoustic microscope. For the calculations here it is assumed that the crack is very deep compared with a wavelength, and the limiting values for a deep crack have been used:

$$T = 0,$$

$$R = 0.4 \exp(\mathrm{i}0.6). \quad (10)$$

The form of the curves is independent of frequency, but to facilitate comparison with the experimental curves in §3 the displacements have been scaled to correspond to a frequency of 215 MHz. Figure 3*b* is for $x_0 = 0$, i.e. the lens directly above the crack. The effect on the reduced $V(z)$ is to decrease the height of the peaks and the depth of the troughs, and to shift the phase by a small amount towards positive z. In terms of the simple ray model this can be thought of as being due to the change in amplitude and phase that the Rayleigh wave suffers on reflection by the crack.

PHILOSOPHICAL TRANSACTIONS OF THE ROYAL SOCIETY A MATHEMATICAL, PHYSICAL & ENGINEERING SCIENCES

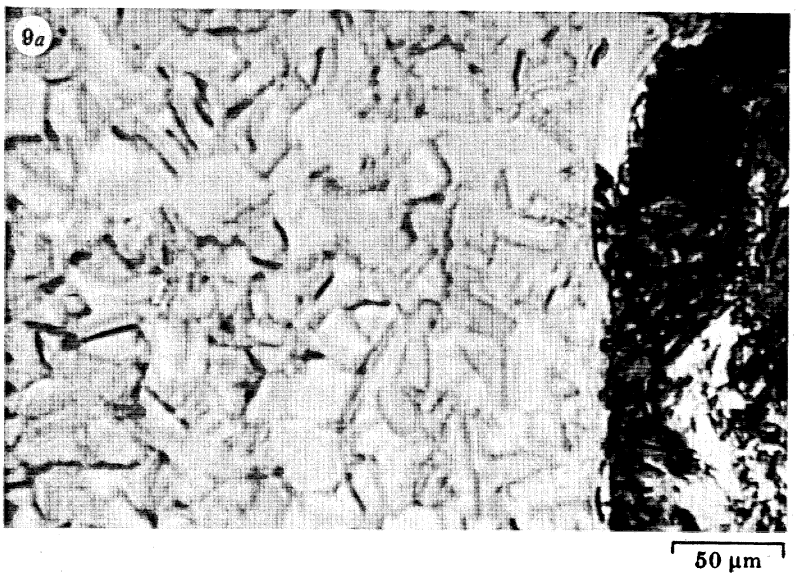

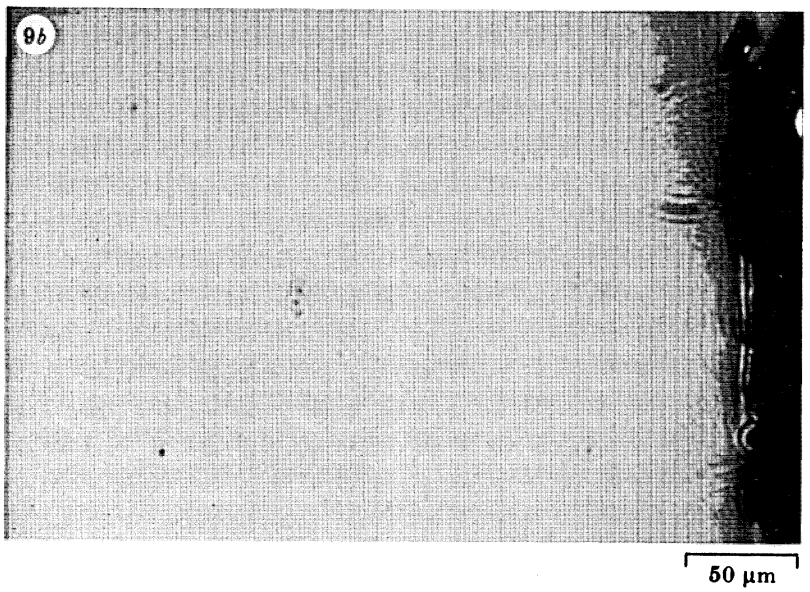

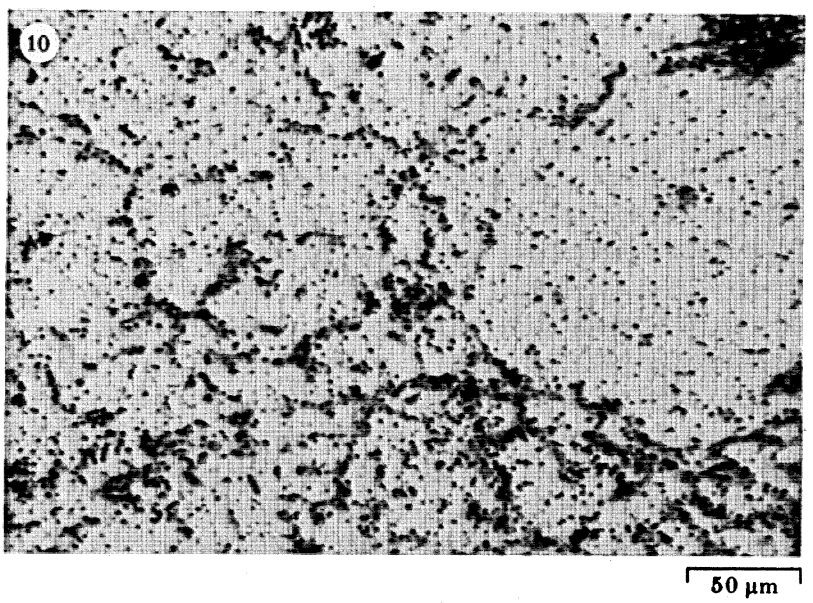

FIGURE 9. Fatigued 316 stainless steel, acoustic micrographs at 0.37 GHz: (*a*) $z = -20$ μm; (*b*) $z = +32$ μm.
FIGURE 10. Zirconia toughened alumina, acoustic image at 0.37 GHz.

PHILOSOPHICAL TRANSACTIONS OF THE ROYAL SOCIETY A MATHEMATICAL, PHYSICAL & ENGINEERING SCIENCES

By choosing a particular value of defocus and calculating the signal as x is varied, a curve can be generated that may be called $V(x)$. This is useful because it represents the line scan that would be obtained when an acoustic microscope is operated at a given defocus and the lens is scanned in the imaging mode. In figure 5 such line scans are shown for the same crack as figures 3 and 4. Figure 5*a* is for $z = 0$, i.e. with the microscope at focus. As is often the case in acoustic microscopy, there is little contrast at focus, although there is a certain amount of ripple present around the crack. This is due to reflection of Rayleigh waves that would otherwise propagate away from the focal region. The periodicity is $\frac{1}{2}\lambda_R$, because for every half wavelength that the lens scans horizontally the path length of such Rayleigh waves changes by one wavelength, and so they come back into the same phase relation with the geometrically reflected waves (Yamanaka & Enomoto 1982). The decay of the oscillations is approximately exponential because of the attenuation of the Rayleigh waves as they propagate along the surface; in these calculations there was no loss in the material itself and so the attenuation is due to leakage of the acoustic power into waves in the fluid.

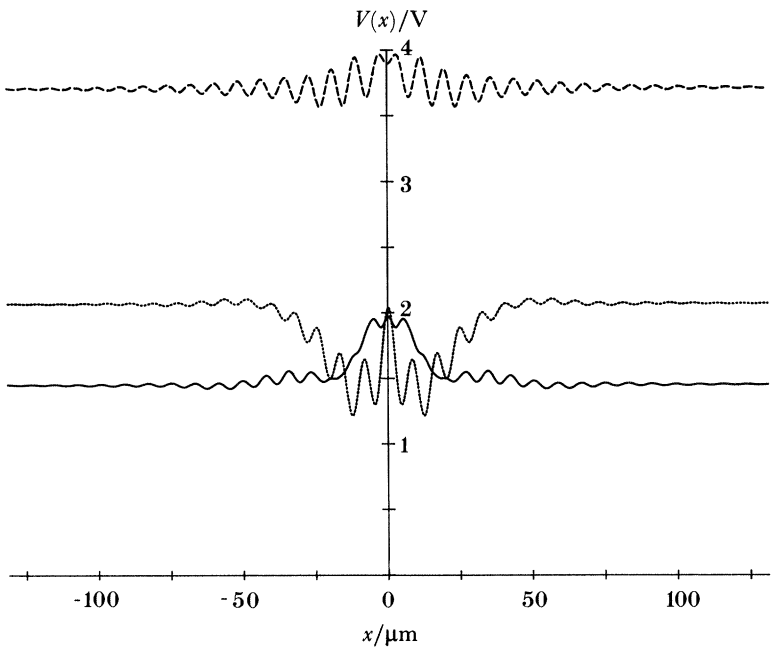

FIGURE 5. Calculated line scans across a crack for the same situation as in figures 3 and 4: (*a*) at focus – – –; (*b*) at 27 μm defocus towards the lens ——; (*c*) at 34 μm defocus · · ·. The vertical scale corresponds to that in figures 3 and 4.

The other two curves in figure 5 show line scans for values of defocus that might be used in obtaining images in the acoustic microscope. Figure 5*b* is for defocus by 27 μm; this corresponds to the first minimum in $V(z)$. Figure 5*c* is for a larger defocus of 34 μm, corresponding to the next maximum. The most prominent feature in these curves is the reversal of contrast as the defocus is changed; this is familiar to anyone with experience of acoustic microscopy, and can be understood in terms of the way that the two curves in figure 3 cross over each other. The calculations also show how the width of the image of a crack is determined primarily by considerations of wave propagation rather than by the width of the crack itself (here assumed to be infinitesimal), and, again, this accounts for observations that are well

known from experimental images such as those in figures 1 and 2, that the width of the image of a fine crack depends primarily upon the imaging conditions rather than on the true width of the crack (Somekh *et al.* 1985).

3. Experimental evaluation

3.1. *Method*

The theory given above is for the two-dimensional situation and, therefore, it must be compared with results obtained with a cylindrical lens. Such lenses have been developed by Kushibiki *et al.* (1981), and they have been extensively evaluated for quantitative work (Kushibiki & Chubachi 1985). The lens used for these measurements had a radius of curvature of 1 mm. The transducer was 1.73 mm^2, giving a line focus approximately 1.73 mm long. The operating frequency was 215 MHz, giving a wavelength in water of $\lambda = 7$ μm. For the specimen, a planar crack was made in a flat piece of glass. An acoustic microscope was set up with the axis of the cylindrical lens accurately parallel both to the surface of the glass and to the plane of the crack. Measurements were made at values of lateral displacement and of defocus corresponding approximately to those used in the calculations of figures 3–5. They were processed by the same procedures, except that this time an experimental $V(z)$ for lead was used, measured during the same experiment.

3.2. *Results*

The results are shown in figures 6–8. They confirm some important features of the theoretical model. The general effect of the crack is to reduce the amplitude of the oscillations, and to shift their phase. When the lens is directly above the crack (figure 6), the amplitude of the oscillations is reduced by about 30% initially, and the phase is shifted by about 1 rad. When the lens is displaced by 10 μm to one side of the crack (figure 7*b*; the Rayleigh wavelength is *ca.* 14 μm), the reduction in the amplitude of the oscillations is considerably greater. When

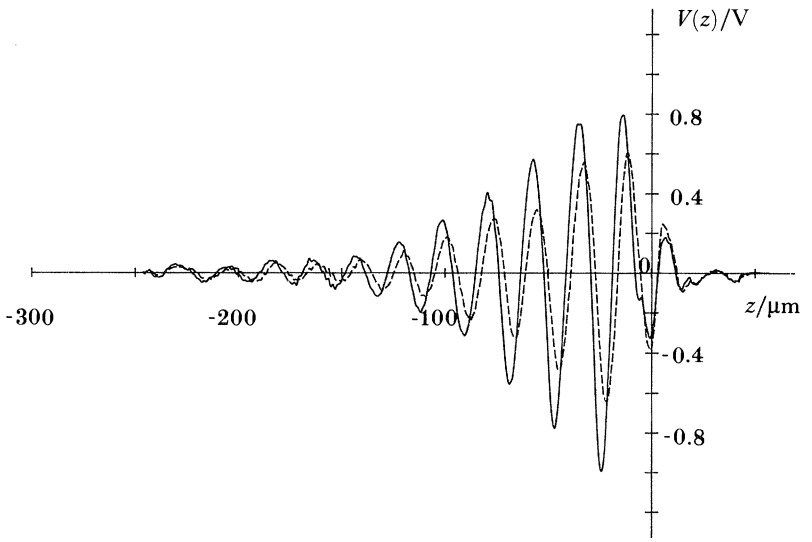

Figure 6. Experimental reduced $V(z)$ curves for glass at 215 MHz: (*a*) defect free ——; (*b*) directly over a crack – – –. (The vertical scale is arbitrary, but it is the same for figures 6, 7 and 8.)

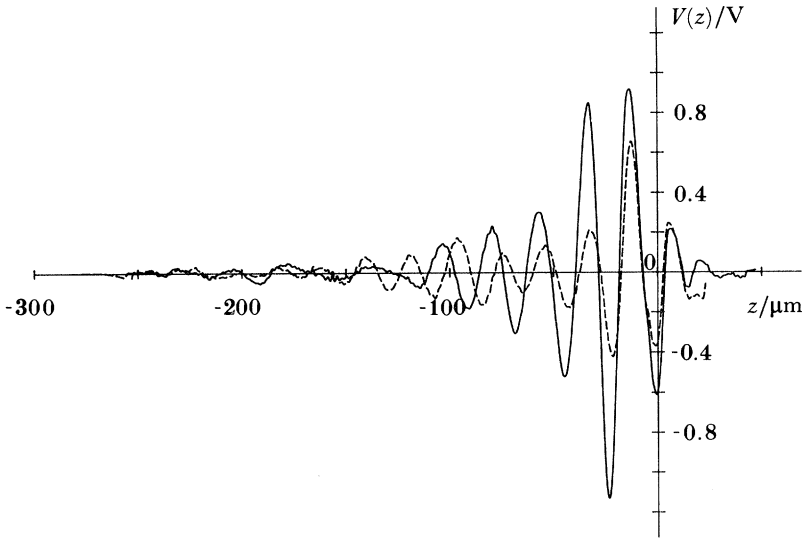

FIGURE 7. Experimental reduced $V(z)$ curves: (a) 10 μm away from a crack – – –; (b) 30 μm away from a crack ——.

the lens is displaced to 30 μm to the side of the crack, the amplitude of the oscillations is initially similar to that for defect-free material, but then becomes affected by the crack at a similar defocus to that predicted theoretically. The experimental line scans across the crack have many features in common with the theoretical $V(x)$; for example at 34 μm defocus there are two subsidiary minima inside the two main minima. Certainly the gross reversal of contrast with defocus is well confirmed.

Of course the agreement between theory and experiment is not perfect. There may be various reasons for this. In the theoretical calculations, the greatest unknowns are the characteristics of the crack and of the lens. Exact values for R and T are not known for a fluid loaded crack

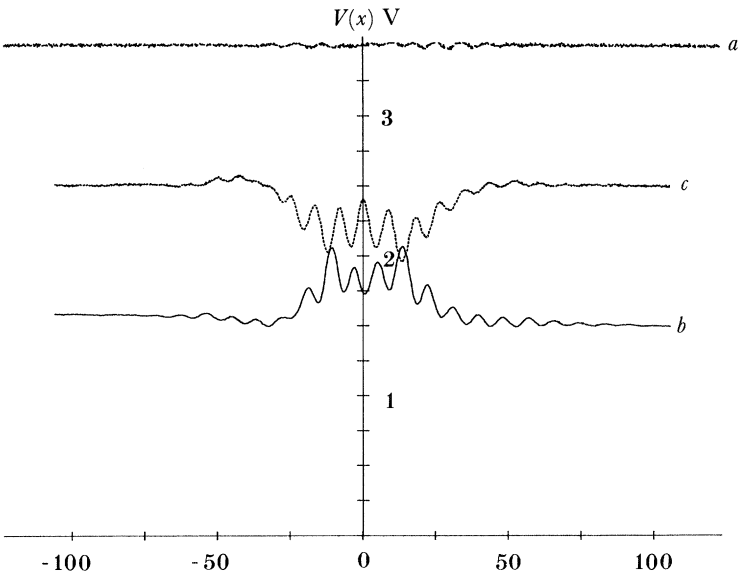

FIGURE 8. Experimental line scans across a crack: (a) at focus – – –; (b) $z = -27$ μm ——; (c) $z = -34$ μm ···.

PHILOSOPHICAL TRANSACTIONS OF THE ROYAL SOCIETY A MATHEMATICAL, PHYSICAL & ENGINEERING SCIENCES

with near-field excitation. Whereas the method of reducing $V(z)$ has been well tried for determining the velocity and attenuation of a Rayleigh wave, it may need further justification for evaluating scattering. On the experimental side, it is extremely difficult to be sure that a crack is smooth and flat to better than 1 μm, and that the two sides are the same height, over a length of more than 1 mm. The lack of perfect symmetry in the curves of figure 8 gives a measure of the difficulty of reproducing ideal conditions in an experiment at these frequencies, and the difference in the relative heights of the curves in figures 5 and 8 reflects the great sensitivity of both theory and experiment to small changes in z. Nevertheless, when all these considerations are taken into account, it appears that the theory does give a substantially accurate account of the experimental phenomena. The theory and the experimental results presented here both apply to two-dimensional situations. The theory could be extended to apply to three dimensions by using calculations that have been performed for Rayleigh waves incident on a surface crack at any angle (Angel & Achenbach 1984). This would enable a full account to be given of the actual images that are obtained in the acoustic microscope with a spherical lens. But it is found, in general, that all the qualitative features of images of cracks are well explained by the two-dimensional theory. Indeed, one of the roles of theory is to guide experiments, and an example will be given in the next section of how the theory has predicted what the optimum conditions should be for imaging cracks where strong grain-boundary contrast is present.

4. Practical applications

4.1. *Fatigue cracks*

The acoustic microscope is particularly sensitive to fatigue cracks in their early stages of growth. An example of an image of fatigue cracks was shown in figure 1. It may be noted in parentheses that figure 1*a*, like some of the other acoustic images presented here, did not show Rayleigh-wave interference fringes parallel to the cracks; these are rarely seen in images of aluminium alloys or in many ceramics, they tend to appear more strongly in materials such as glass, semiconductors and stainless steel. It is believed that such observations can be accounted for in terms of the theory presented here, but the details remain to be worked out. The acoustic microscope can also give contrast from grain structure (Somekh *et al.* 1984). Aluminium has a relatively low crystal anisotropy, and that is why grain structure is scarcely visible in figure 1*a*. Other materials, however, may give strong grain contrast, and in some cases, notably stainless steel, there may also be strong contrast from the grain boundaries too. One of the predictions of a more general version of the theory presented here (Somekh *et al.* 1985) is that contrast from grain boundaries will almost disappear at positive defocus, whereas cracks will remain visible.

An acoustic image of a specimen of 316 stainless steel is shown in figure 9*a*, plate 2. This specimen had been fatigued in torsion in order to investigate the earliest stages of short-crack growth (de los Rios *et al.* 1985). This image was obtained at negative defocus, and contrast is present from both grain structure and from fatigue cracks. However, the grain boundary contrast is so strong that it is not easy to distinguish the cracks in this picture. In figure 9*b* the specimen has been moved away from the lens to make the defocus positive, and the result is that, as predicted, the grain contrast is greatly reduced and two or three cracks are now revealed more prominently. Once the cracks have been seen, they can be more readily identified by their characteristic fringe pattern in the negative defocus image of figure 9*a*.

PHILOSOPHICAL TRANSACTIONS OF THE ROYAL SOCIETY A MATHEMATICAL, PHYSICAL & ENGINEERING SCIENCES

4.2. *Ceramics*

Low-ductility advanced materials, such as engineering ceramics, are able to support little or no plastic deformation. Their fracture toughness is low and the critical defect size that can be tolerated is much smaller than in most alloys. The critical defect size depends, of course, on the material and the application; a typical value might be 30 μm. This is too small to detect by using conventional ultrasonic NDT frequencies, but is within the range of the resolution of the images presented here. Figure 10, plate 2, is an example of an image of a ceramic material; this is a specimen of a zirconia-toughened alumina ceramic. Part of the area shown in the image is relatively sound, but the remainder shows extensive cracking, probably associated with transformation of the zirconia. This specimen was prepared for acoustic microscopy by lapping on a solder wheel with 1 μm diamond paste. There is a possibility that the cracks were introduced during the polishing process, and it will be important to develop very good preparation techniques in order to use acoustic microscopy for metallography of sections of ceramic specimens. This problem, however, may also be turned to advantage and exploited. Machining damage can be a serious source of weakness in ceramics, acoustic microscopy (at a wavelength appropriate to the machined surface topography) may prove a powerful technique for imaging and evaluating cracks in machined ceramic surfaces (Marshall *et al.* 1983).

4.3. *Prospects*

The acoustic microscope can give strong contrast in images of surface cracks. The theory that has been developed gives a good account of the mechanism responsible for this contrast. There is now increasing interest in the use of acoustic microscopy for quantitative work, as well as for imaging, so that a feature of interest in an acoustic image can be measured by using both $V(z)$ and line scans. An important challenge is therefore to characterize cracks quantitatively. This has been demonstrated on a larger scale, by using reflections from Rayleigh waves launched from discrete transducers (Marshall *et al.* 1983); it remains to be done in the acoustic microscope with the resolution of the images presented here. Acoustically the crack is characterized by the two parameters R and T; these depend on the depth of the crack and on the contact conditions between the faces. The ripple of half Rayleigh wavelength in $V(x)$ depends primarily on R, while the magnitude of the central disturbance in $V(x)$, and also the perturbation in the oscillations in $V(z)$ depend on both R and T. Thus, a combination of measurements should yield information about these two parameters that will give information about the geometry of the crack; considerably more information may be available if measurements can be made at more than one frequency.

The facilities for the use of the line focus lens, and the implementation of the processing techniques were established while J. K. was an SERC Visiting Fellow at Oxford in 1984. SERC also supported J. M. R. with a CASE studentship, sponsored by GEC Hirst, and M. G. S. with a postdoctoral research fellowship. The fatigue of stainless steel is being studied in collaboration with Dr E. R. de los Rios and Professor K. J. Miller. Figure 10 was photographed by Dr P. J. Burnett in collaboration with Dr R. Stevens.

PHILOSOPHICAL TRANSACTIONS OF THE ROYAL SOCIETY A MATHEMATICAL, PHYSICAL & ENGINEERING SCIENCES

References

Achenbach, J. D., Gautesen, A. K. & Mendelsohn, D. A. 1980 Ray analysis of surface-wave interaction with an edge crack. *IEEE Trans. Sonics Ultrasonics* **SU-27**, 124–129.

Angel, Y. C. & Achenbach, J. D. 1984 Reflection and transmission of obliquely incident Rayleigh waves by a surface crack. *J. acoust Soc. Am.* **75**, 313–318.

Bertoni, H. L. 1984 Ray-optical evaluation of $V(z)$ in the reflection acoustic microscope. *IEEE Trans. Sonics Ultrasonics* **SU-31**, 105–116.

Briggs, G. A. D. 1985 *An introduction to scanning acoustic microscopy*. Oxford University Press and the Royal Microscopical Society.

de los Rios, E. R., Mohamed, J. & Miller, K. J. 1985 A micro-mechanics analysis for short fatigue crack growth. *Fatigue Fract. Engng Mater. Struct.* **8**, 49–63.

Hadimioglu, B. & Quate, C. F. 1983 Water acoustic microscopy at suboptical wavelengths. *Appl. phys. Lett.* **43**, 1006–1007.

Ilett, C., Somekh, M. G. & Briggs, G. A. D. 1984 Acoustic microscopy of elastic discontinuities. *Proc. R. Soc. Lond.* A **393**, 171–183.

Kushibiki, K. & Chubachi, N. 1985 Material characterization by line-focus-beam acoustic microscope. *IEEE Trans. Sonics Ultrasonics* **SU-32**, 189–212.

Kushibiki, J., Ohkubo, A. & Chubachi, N. 1981 Linearly focused acoustic beams for acoustic microscopy. *Electron. Lett.* **17**, 520–522.

Lemons, R. A. & Quate, C. F. 1979 Acoustic microscopy. In *Physical acoustics* (ed. W. P. Mason & R. N. Thurston), vol. 14, pp. 1–92. London: Academic Press.

Marshall, D. B., Evans, A. G., Khuri Yakub, B. T., Tien, J. W. & Kino, G. S. 1983 The nature of machining damage in brittle materials. *Proc. R. Soc. Lond.* A **385**, 461–475.

Quate, C. F., Atalar, A. & Wickramasinghe, H. K. 1979 Acoustic microscopy with mechanical scanning – a review. *Proc. IEEE* **67**, 1092–1114.

Smith, I. R., Harvey, R. A. & Fathers, D. J. 1985 An acoustic microscope for industrial applications. *IEEE Trans. Sonics Ultrasonics* **SU-32**, 274–288.

Somekh, M. G., Briggs, G. A. D. & Ilett, C. 1984 The effect of anisotropy on contrast in the scanning acoustic microscope. *Phil. Mag.* **49**, 411–415.

Somekh, M. G., Bertoni, H. L., Briggs, G. A. D. & Burton, N. J. 1985 A two-dimensional imaging theory of surface discontinuities with the scanning acoustic microscope. *Proc. R. Soc. Lond.* A **401**, 29–51.

Weglein, R. D. 1979 A model for predicting acoustic material signatures. *Appl. phys. Lett.* **35**, 215–217.

Yamanaka, K. & Enomoto, Y. 1982 Observation of surface cracks with scanning acoustic microscope. *J. appl. Phys.* **53**, 846–850.

Discussion

C. B. Scruby (*AERE Harwell, Oxfordshire, U.K.*). Some of the most interesting features of the image are produced by the interference of normally reflected and mode-converted Rayleigh waves. Could the image contrast be enhanced by blanking off other parts of the lens which do not contribute to either of these rays, and has anyone explored this possibility?

G. A. D. Briggs. Experiments have been performed to investigate the effect of blanking out annular regions of the lens aperture, but that was to remove the Rayleigh waves rather than to enhance them (Nikoonahad *et al.* 1983). Blanking off other parts of the lens might enhance the Rayleigh-wave contrast, but this is what is, in effect, achieved by defocusing, because interference at the transducer then greatly reduces the contribution from rays at other angles of incidence (Atalar 1979). There is considerable scope for making interesting measurements by using special transducer configurations and electrical reference signals, but the practical problems at high frequencies should not be underestimated.

References

Atalar, J. 1979 A physical model for acoustic signatures. *J. appl. Phys.* **50**, 8237–8239.

Nikoonahad, M., Sivaprakasapillai, P. & Ash, E. A. 1983 Rayleigh wave suppression in reflective acoustic microscopy. *Electron. Lett.* **19**, 906–908.

PHILOSOPHICAL TRANSACTIONS OF THE ROYAL SOCIETY A MATHEMATICAL, PHYSICAL & ENGINEERING SCIENCES

D. P. Almond (*School of Materials Science, University of Bath, U.K.*). What are the values of the surface-wave reflection and transmission coefficients used in Dr Briggs's analysis?

G. A. D. Briggs. The values that we have used are given in (10). These values do not arise out of the theory; they must be supplied externally. Here, and in related work (Somekh *et al.* (1985), where the effect of changes in the depth of the crack are also considered) we have used values computed by Achenbach and his colleagues. Those results were calculated for far-field excitation in the absence of fluid loading, and there is a great need for a better evaluation of the scattering parameters when there is near-field excitation by waves incident from the fluid. The effect on $V(z)$ is quite sensitive to the parameters used in the calculation, and this is good from the point of view of the use of the technique experimentally to characterize cracks.

R. B. Thompson (*Ames Laboratory, Iowa State University, Ames, Iowa, U.S.A.*). In Dr Briggs's talk, it seemed to be implied that the position of a surface crack with respect to the 'footprint' of the insonifying wave on the sample surface was an important parameter. Was he saying that detection of cracks only occurs when a crack is within the footprint so that it disturbs a Rayleigh wave propagating from one side of the beam to the other? Would it not also be possible for a Rayleigh wave to propagate away from the 'footprint', be reflected from a crack, and return to the beam region for detection?

G. A. D. Briggs. Provided that there is some reflection of the Rayleigh wave by the crack (as there usually is) then even if the crack is outside the zone of the incident beam there can be some effect from the crack. Some of these effects can be seen in the curves of $V(z)$ and $V(x)$. For the situation in figures 4*b* and 7*b* with the lens 30 μm to one side of the crack the crack would be included in the beam when $z < -50$ μm, but there are variations compared with figures 3*a* and 6*a* for greater values of z. This is especially noticeable in the theoretical curves in the positive range $0 < z < 50$ μm, which corresponds to excitation quite close to the crack itself. Similarly, in the experimental and theoretical $V(x)$ curves the Rayleigh-interference ripple is present even when the crack is outside the zone of the beam (this is about 7 μm across at focus, increasing to 20 μm when $z = -34$ μm), and again this must be due to reflection from the crack. In an acoustic micrographs of surface cracks these ripples would appear as fringes parallel to the cracks; as mentioned in §4.1, these are seen in many, but not all materials.

Cracks can be distinguished from grain boundaries in figure 9 because grain boundaries are detected primarily by the change in velocity of transmitted surface waves, whereas cracks give contrast because of reflection and loss of transmission. At positive defocus only the reflection contrast mechanism can operate and, because reflection from grain boundaries is much weaker than from cracks, cracks give much stronger contrast. At positive defocus waves reflected from a crack can return to the transducer only when the crack is outside the incident beam. This might be expected to give a double image from a crack, one each side, and some evidence for this can be seen in the pattern of the fringes of the middle crack in figure 9*b*.

H. N. G. Wadley (*A*163, *Materials Building* 223, *NBS, Gaithersburg, Maryland, U.S.A.*). For the last four or five years there has been a good deal of interest in the quantitative determination of elastic constants from the $V(z)$ curve, an elastic microprobe modality if you like. Dr Briggs made no mention of such potential and I wonder if this reflects unanticipated problems with the analysis?

PHILOSOPHICAL TRANSACTIONS OF THE ROYAL SOCIETY A MATHEMATICAL, PHYSICAL & ENGINEERING SCIENCES

G. A. D. Briggs. Considerable progress has been made in this area, which is indeed a very important one. If the phase of $V(z)$ is measured then it is possible to invert the transform described by (3) and, once the lens has been characterized, determine the reflectance function of the specimen surface. This has been achieved with impressive accuracy at frequencies of 10 MHz (Liang *et al.* 1985) and even higher. Above 50 MHz accurate measurements of phase are harder, and analysis can be performed on the measurements of $|V(z)|^2$ that are obtained from the standard-square-law diode detector of an acoustic microscope. This technique has been mainly developed using a cylindrical line-focus lens at 225 MHz, and it has been extensively tested (Kushibiki & Chubachi 1985). It is this technique that we have adapted for the measurements on cracks reported here. The cylindrical lens has the advantage of azimuthal resolution for anisotropic materials, but at the expense of spatial resolution. By using similar analysis techniques on $V(z)$ measured with a spherical imaging lens in the acoustic microscope, the velocity and attenuation of Rayleigh waves may be determined at a given point on an acoustic micrograph with spatial resolution of a few micrometres, and this is of enormous significance for quantitative image interpretation.

Additional reference

Liang, K. K., Kino, G. S. & Khuri-Yakub, B. T. 1985 Materials characterization by the inversion of $V(z)$. *IEEE Trans. Sonics Ultrasonics* **SU-32**, 213–224.

PHILOSOPHICAL TRANSACTIONS OF THE ROYAL SOCIETY A MATHEMATICAL, PHYSICAL & ENGINEERING SCIENCES

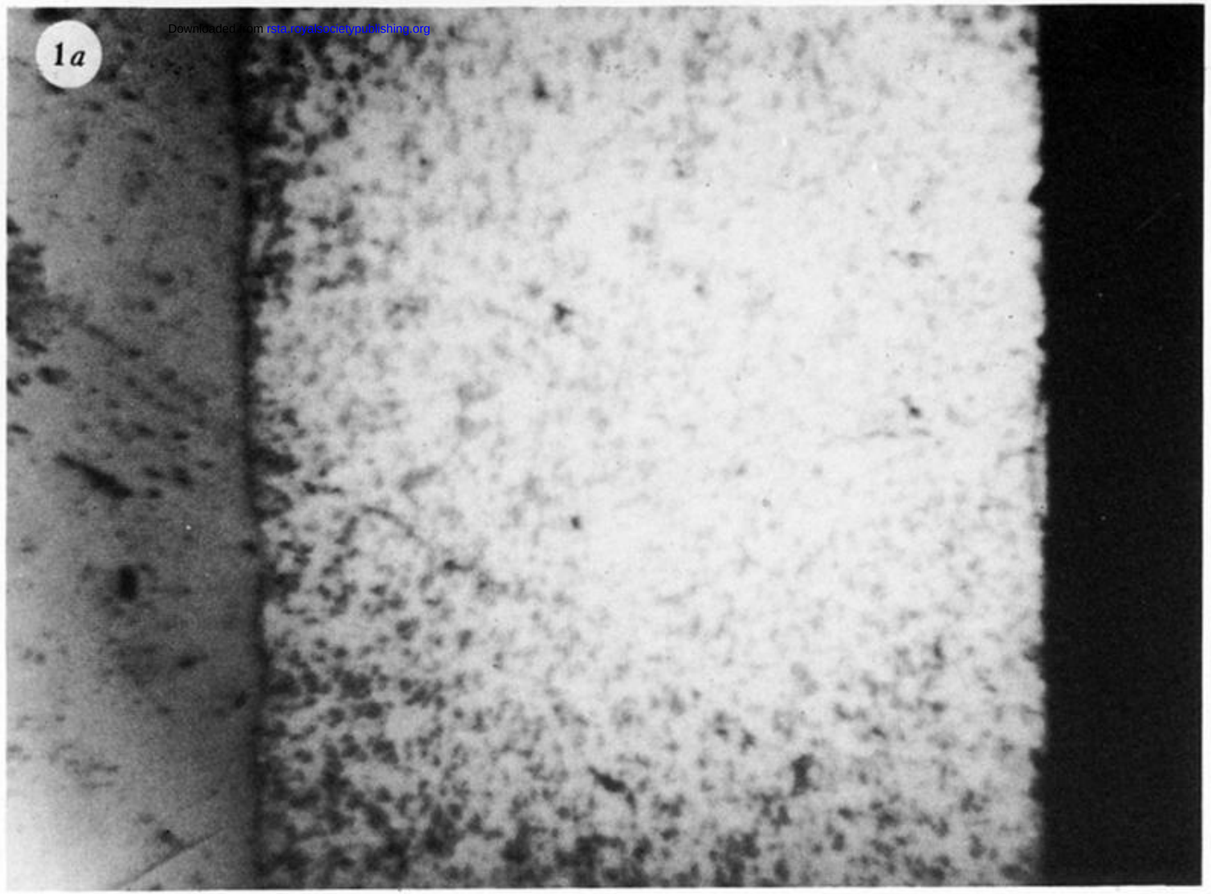

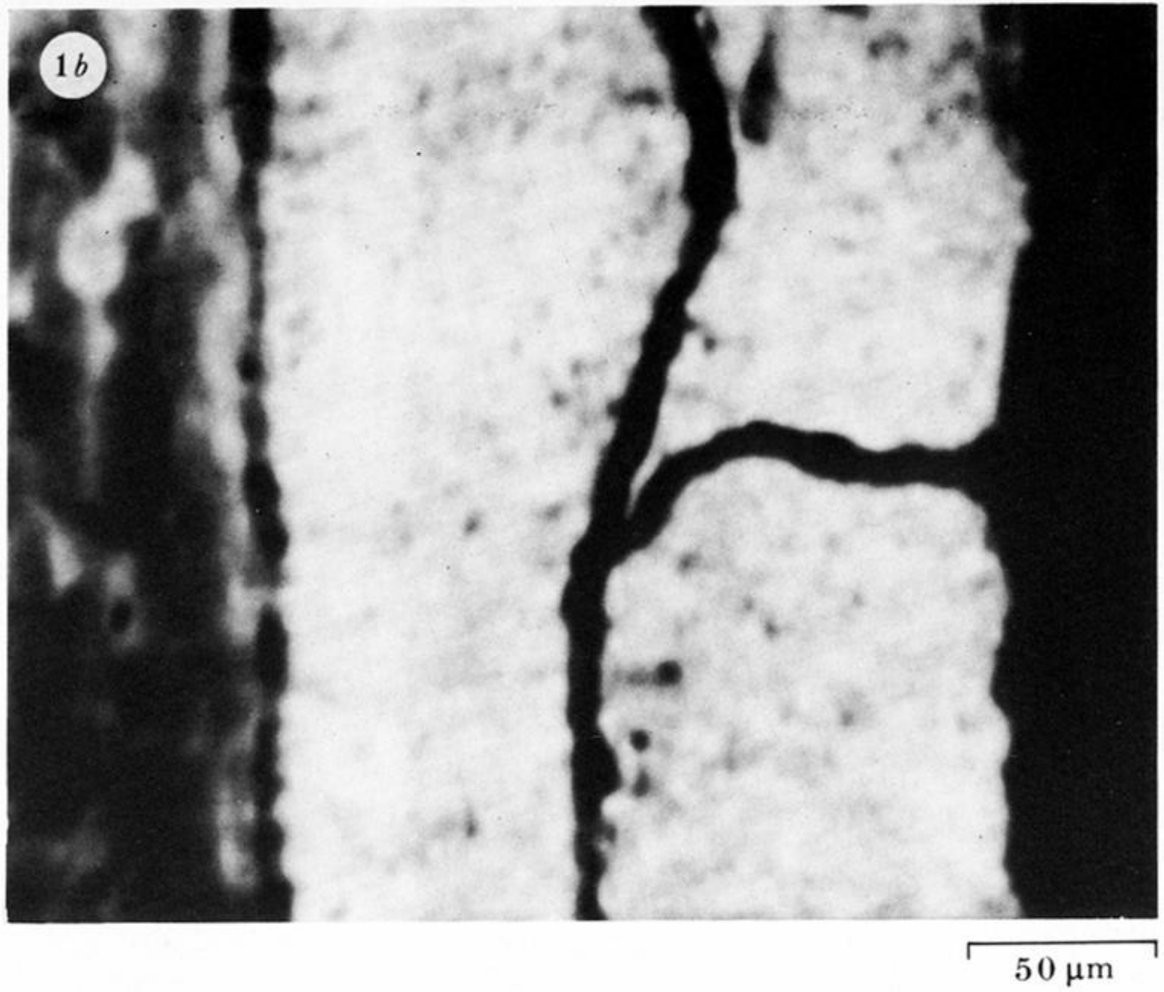

FIGURE 1. A plain bearing that has been tested for fatigue failure. The optical (*a*) and acoustic (*b*) images are of the same area at the same magnification. At the left is the steel substrate, in the centre is the Al–20 % Si bearing alloy containing the fatigue cracks. The acoustic image was taken at 0.73 GHz.

PHILOSOPHICAL TRANSACTIONS OF THE ROYAL SOCIETY A MATHEMATICAL, PHYSICAL & ENGINEERING SCIENCES

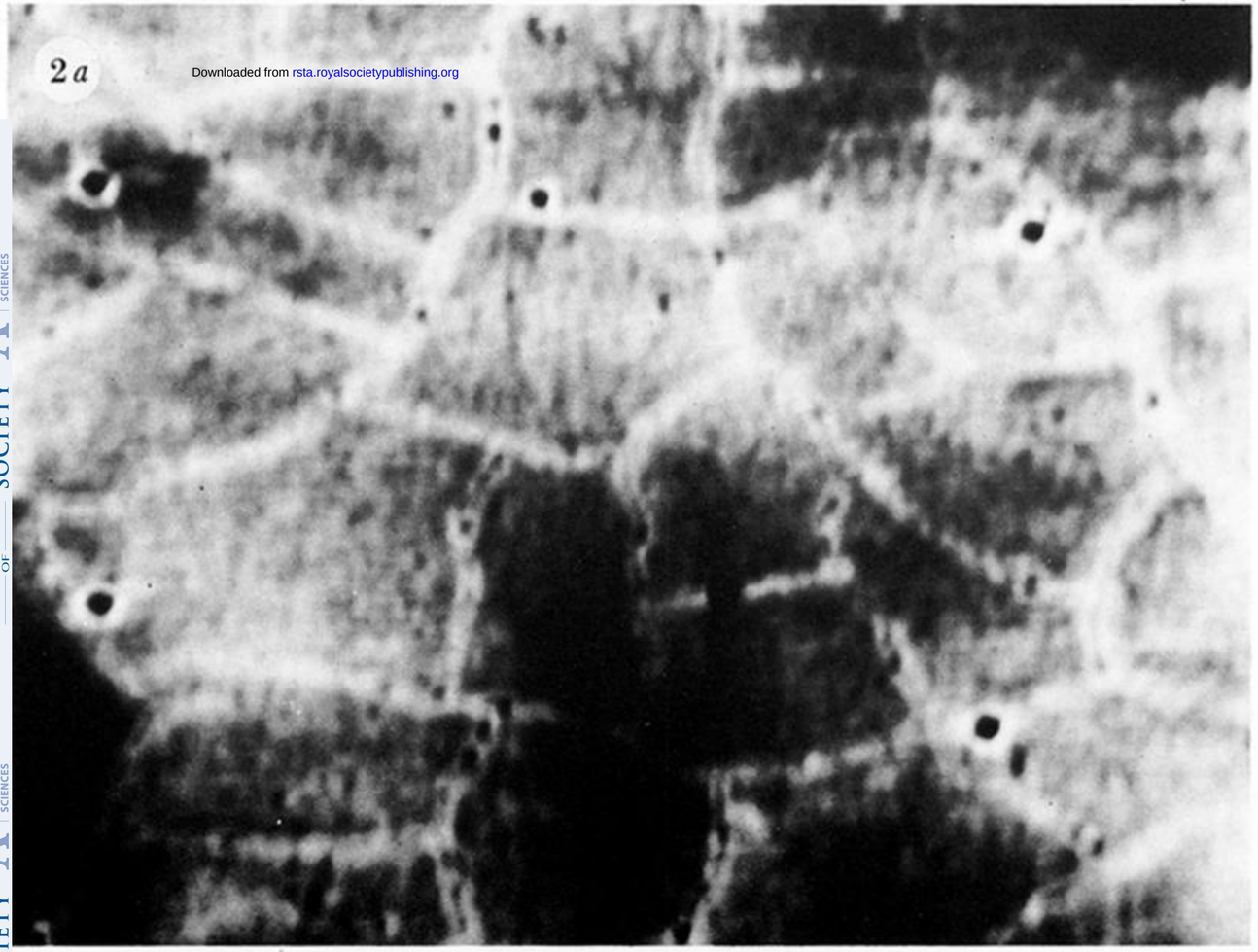

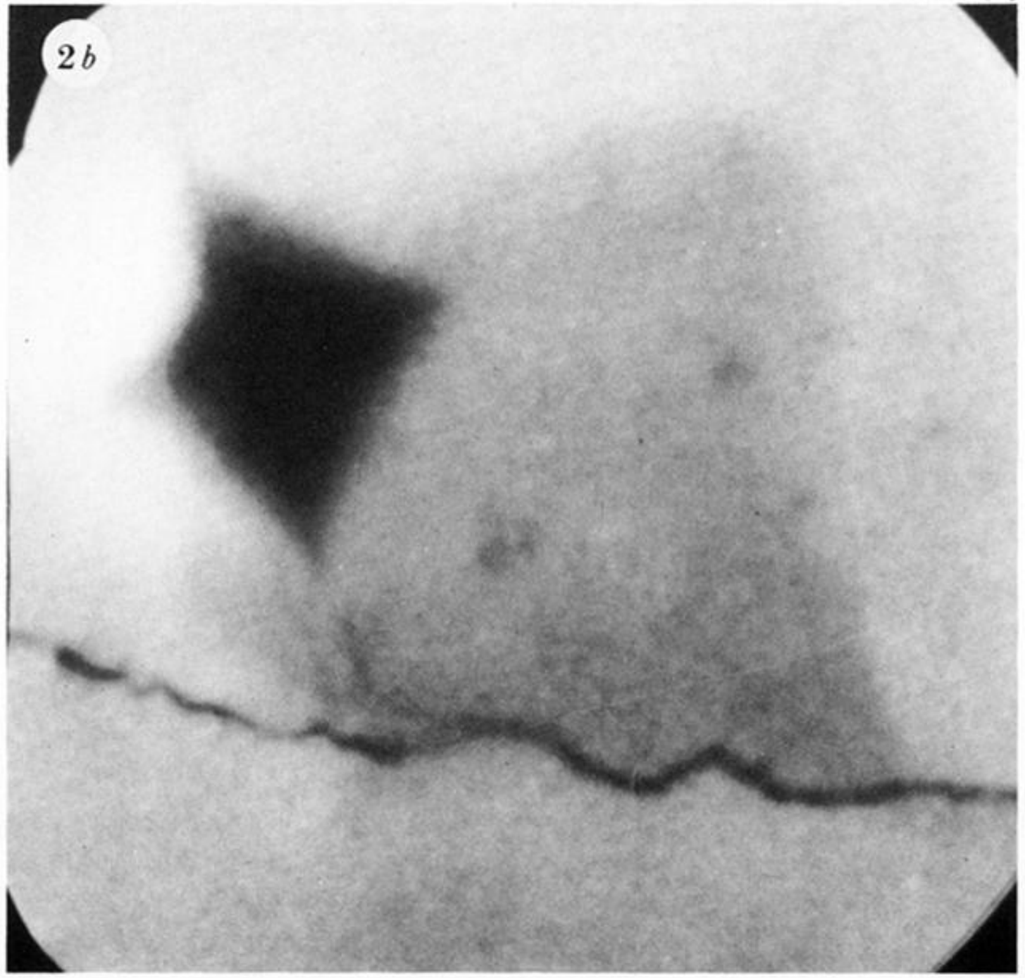

FIGURE 2. A hard metal cutting tool, coated with TiN. A region in the top centre of the acoustic image (*a*) is shown at 25 times greater magnification in the SEM image (*b*). The acoustic image was taken at 0.73 GHz, at this frequency the wavelength in water is 2 μm.

PHILOSOPHICAL TRANSACTIONS OF THE ROYAL SOCIETY A MATHEMATICAL, PHYSICAL & ENGINEERING SCIENCES

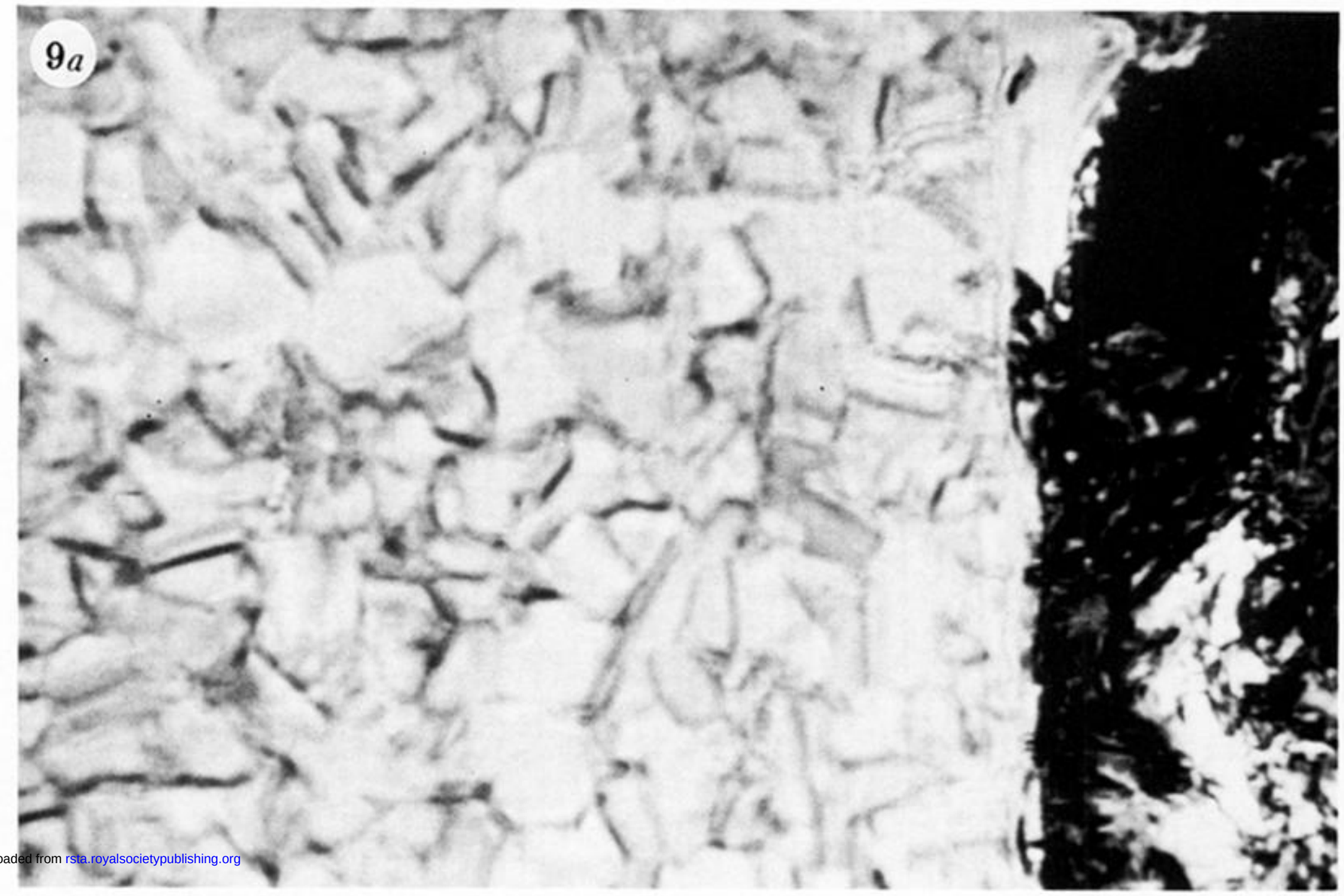

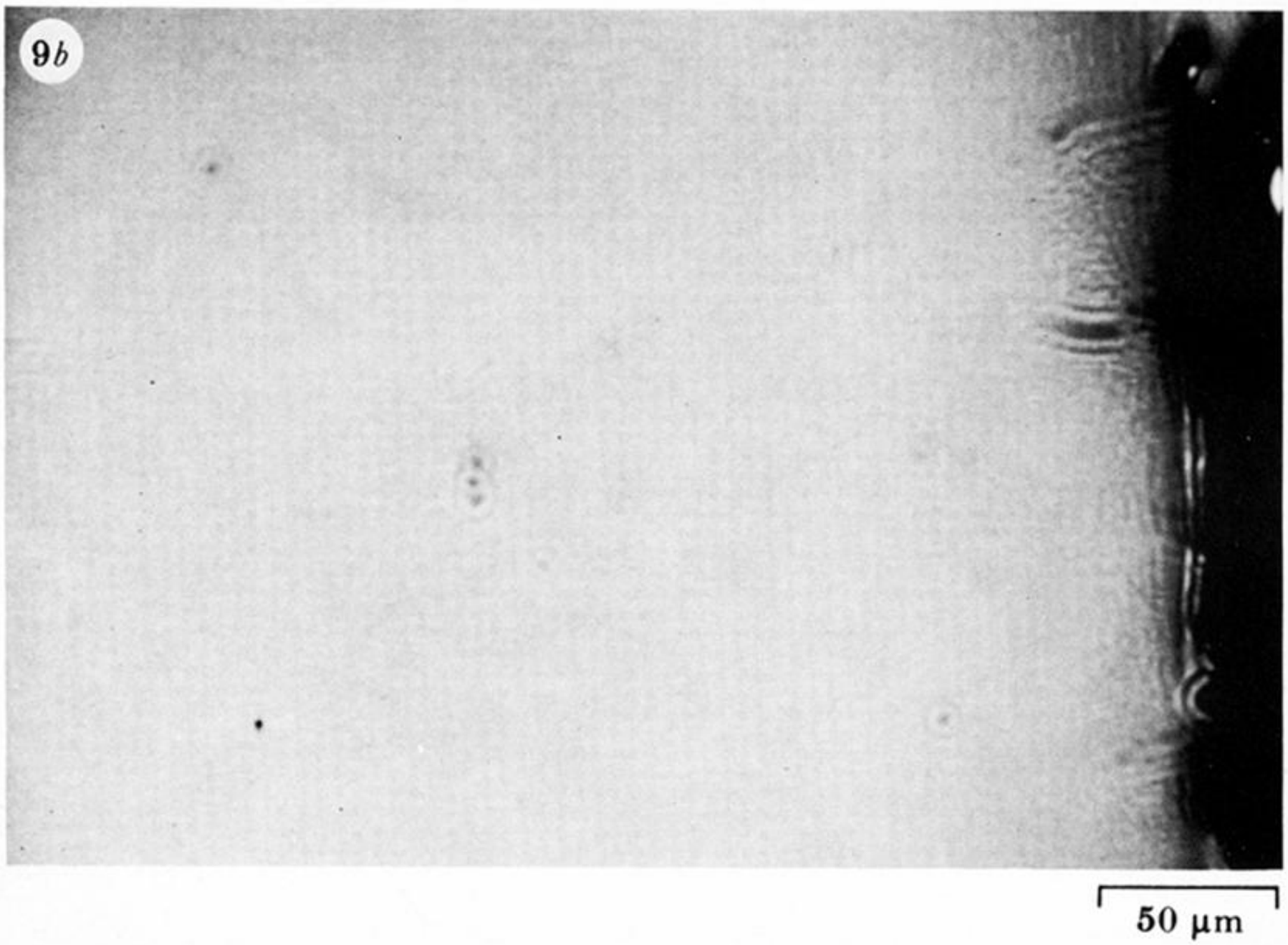

FIGURE 9. Fatigued 316 stainless steel, acoustic micrographs at 0.37 GHz: (*a*) $z = -20$ μm; (*b*) $z = +32$ μm.

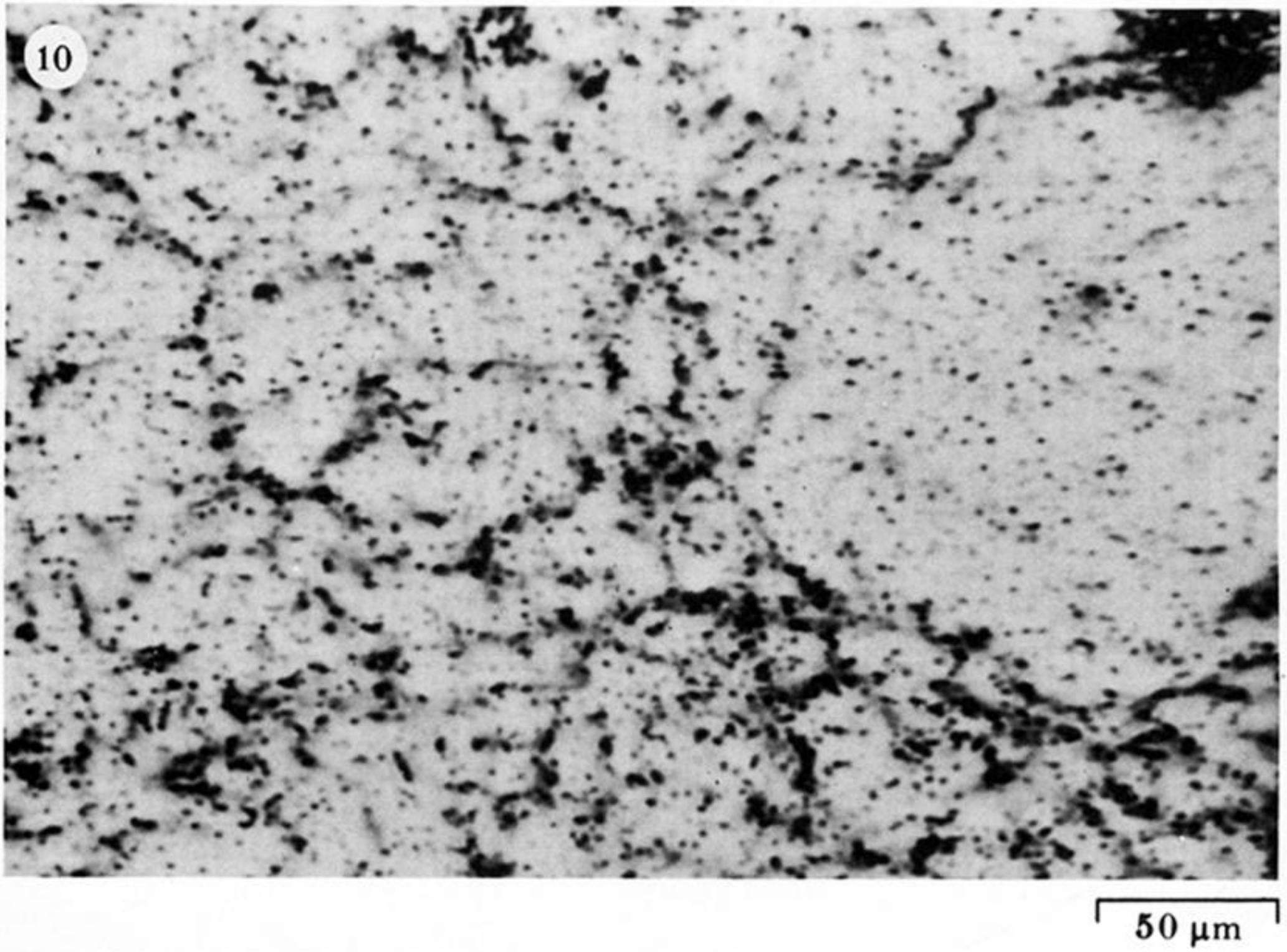

FIGURE 10. Zirconia toughened alumina, acoustic image at 0.37 GHz.

PHILOSOPHICAL TRANSACTIONS OF THE ROYAL SOCIETY A MATHEMATICAL, PHYSICAL & ENGINEERING SCIENCES